

## Article

# Source, Distribution and Transformation of Organic Matter in a Subtropical Karst Reservoir

Jianhong Li <sup>1</sup>, Tao Zhang <sup>2,\*</sup>, Junbing Pu <sup>2</sup>, Xiangling Tang <sup>3</sup>, Yincai Xie <sup>1</sup>  and Qiong Xiao <sup>1</sup>

<sup>1</sup> Key Laboratory of Karst Dynamics, Ministry of Natural Resources & Guangxi, Institute of Karst Geology, Chinese Academy of Geological Sciences, Guilin 541004, China; jianhonglikarst@163.com (J.L.); xiaoqiong-8423@163.com (Q.X.)

<sup>2</sup> Chongqing Key Laboratory of Wetland Science Research of the Upper Reaches of the Yangtze River & Chongqing Key Laboratory of Surface Process and Environment Remote Sensing in the Three Gorges Reservoir Area, School of Geography and Tourism, Chongqing Normal University, Chongqing 401331, China

<sup>3</sup> Guilin University of Technology Institute of Earth Science, Guilin 541004, China

\* Correspondence: tao21mi@163.com

**Abstract:** In order to improve the understanding of the global carbon cycle and the stability of karst carbon sinks, it is necessary to better understand the source, distribution and transformation characteristics of organic matter (OM) in aquatic ecosystems. Here, stable isotope ratios ( $\delta^{13}\text{C}$  and  $\delta^{15}\text{N}$ ), elemental analysis (C/N ratios), and lipid biomarkers were analyzed for dissolved organic matter (DOM) ( $<0.7\ \mu\text{m}$ ), particulate organic matter (POM) ( $>0.7\ \mu\text{m}$ ) of water, and organic matter from sediment cores (SCOM) to identify the sources, distribution, and transformation of OM in a subtropical karst reservoir. The results showed that short-chain (C14–20) n-alkyl lipids were more abundant than long-chain (C21–34) n-alkyl lipids in both the DOM and SCOM samples, indicating that bacteria were the primary sources of these lipids, while terrestrial organic matter (OM) made only a minor contribution to the n-alkyl lipid pool, and aquatic plants (macrophytes) OM contributed major contribution to the n-alkyl lipid pool in POM. microbial activity and lipid degradation were more pronounced in the DOM. Furthermore, terrigenous and macrophyte-derived lipids were found to be more abundant in POM than in DOM and SCOM, suggesting that they are relatively resistant to degradation compared with phytoplankton-derived OM.



**Citation:** Li, J.; Zhang, T.; Pu, J.; Tang, X.; Xie, Y.; Xiao, Q. Source,

Distribution and Transformation of Organic Matter in a Subtropical Karst Reservoir. *Water* **2023**, *15*, 3255.

<https://doi.org/10.3390/w15183255>

Academic Editor: Achim A. Beylich

Received: 1 August 2023

Revised: 8 September 2023

Accepted: 9 September 2023

Published: 13 September 2023



**Copyright:** © 2023 by the authors. Licensee MDPI, Basel, Switzerland. This article is an open access article distributed under the terms and conditions of the Creative Commons Attribution (CC BY) license (<https://creativecommons.org/licenses/by/4.0/>).

**Keywords:** dissolved organic matter; particulate organic matter; water; karst reservoir; lipid biomarkers

## 1. Introduction

Organic matter (OM) in the natural environment plays an important role in aquatic ecosystems, which operate as a shuttle for the long-range transport of chemicals and serve as the source of carbon, nutrients, and energy for all ecosystems [1,2]. Additionally, due to its high organic carbon content, OM is actively involved in global carbon balance. Assessing the global carbon balance has been one of the most important scientific issues in global change research [3]. According to geochemical characteristics, OM can be separated into autochthonous and allochthonous organic matter, which are associated with phytoplankton primary production and terrestrial plants and soil, endogenous, respectively [4–6]. Previous studies have demonstrated that aquatic phototrophs transform inorganic carbon (DIC) formed by carbonate weathering into relatively stable organic carbon (OC) through photosynthesis, which is a key process for the stability of karst carbon sink [7–10]. Therefore, in order to improve our understanding of the global carbon cycle and the stability of karst carbon sinks, it is necessary to gain a better understanding of the sources, distribution, and transformation characteristics of organic carbon in aquatic ecosystems.

The ratios of autochthonous and allochthonous OMs are quite complex because of their mixing [9], but some methods can be used to estimate OM composition. The spectroscopic indices method, elemental analysis (C/N ratios), isotope ratios analysis ( $\delta^{13}\text{C}$

and  $\delta^{15}\text{N}$ ), and the molecular biomarker approach are the most reliable methods to identify the sources and the transformation processes of OM [5,9]. Each method presents benefits/merits and disadvantages in the application [5]. Although the spectroscopic indices, which are calculated based on UV-Vis absorption and fluorescence spectra, can be measured rapidly on-site and are based on a non-destructive and reagent-free analysis requiring much fewer pre-treatments [5,11], this optical approach is constrained to color and fluorescent DOM only and can be related to the bulk DOM properties by correlation analyses. The determination of spectroscopic indices is affected by solution chemistry, such as pH, OM concentration, and the metal complexes [5]. Although isotope ratio analysis ( $\delta^{13}\text{C}$  and  $\delta^{15}\text{N}$ ) and elemental analysis (C/N ratios) have become increasingly popular for inferring the sources and the transformation processes of organic carbon, they are difficult to identify OM sources in complex systems due to the overlaps in the stable isotopic signatures of source materials [12] and the highly variable of C/N ratios, which influenced by remineralization and decomposition processes [5,9]. Previous lipids biomarkers offer the identification of OM sources with a higher level of accuracy [5,13]. Among the lipid biomarkers, n-alkanes, fatty acids and sterols play an important role in tracing the source, migration and change of organic matter in the ecological environment due to their different structures [14] and different degradation degrees [15,16]. As an example, the autochthonous aquatic sources of SOM versus allochthonous terrestrial sources can use alkanes, long-chain alcohols, n-alkan-2-ones, terpenes/terpenoids and sterols to discriminate [17].

The predominance of the short-chain n-alkanes (<C<sub>20</sub>) is characteristic of bacteria, algae, and/or planktons as well as other possible marine sources, whereas the long-chain n-alkanes (C<sub>25</sub>~C<sub>35</sub>) with a strong odd-to-even carbon are the characteristics of terrestrial sources [5,17,18]. Long-chain saturated fatty acids are mainly derived from terrestrial organic sources (vascular plants), whereas short-chain saturated fatty acids indicate the presence of aquatic sources (algal and microbial) [5,9,19]. However, the molecular biomarker approach also has obvious limitations. The first limitation is their ubiquity, leading to potentially equivocal source assignments. The second limitation is their sensitivity to diagenetic effects. Another limitation is related to the representativeness of bulk OM biomarker molecules. Biomarker molecules typically are a very small fraction of the total mixture and may not be representative of the whole, even though they convey important information about details of individual sources and diagenetic pathways [5,20]. Due to the complex composition and the heterogeneous sources of OM in aquatic ecosystems, which affect the accuracy of the simulation results, the application of multi-proxies and multi-models is critical for accurately estimating the source of OM and the development trend of future research [6,16].

Lakes and reservoirs are important regional carbon accumulation and transfer stations in terrestrial ecosystems and have attracted greater attention [6,19,21]. The most special of these are the karst reservoirs, which are generally rich in dissolved inorganic carbon (DIC) and have a longer retention time. They provide a well-defined system to understand the conversion mechanism of autochthonous organic matter (OM) and demonstrate the stability of the karst carbon sink [22,23]. Our previous studies in Dalongdong (DLD reservoir) using  $\delta^{13}\text{C}$ ,  $\delta^{15}\text{N}$ , and C/N have suggested that the sources of OC in the sediments were derived from plankton (60.84%), soil (22.93%), wastewater (14.56%), and terrestrial plants (1.67%) [24]. On the other hand, the sources of settling particulate organic carbon (SPOC) in the DLD reservoir were derived from resuspension matter (45.27%), algae (31.57%), domestic sewage (15.91%), and soil (7.24%) [22].

However, our previous studies were not sufficiently systematic. OM exists in the form of particulate organic matter (POM), dissolved organic matter (DOM) and sedimentary organic matter (SOM). Like many other studies, our previous study only discussed and analyzed one type of organic matter using simplex isotope ratio proxies [22]. However, there is limited relevant information on all types of organic matter for the karst reservoir system. These mutually dependent processes should be discussed together because con-

sidering the interactions between water, rock, gas, and organisms as a whole is necessary to understand the conversion mechanism of autochthonous organic matter and the transformation relationship of organic matter in different states. Based on the analysis of the existence and distribution of lipid biomarkers, the author can summarize the different degradation modes of lipid biomarkers and then reveal the relationship and significance of different degradation modes of lipid biomarkers with the study of the global carbon cycle and climate change. In this study, we examined the distribution of lipid biomarkers, specifically n-alkanes and fatty acids, in both DOM, POM, and SCOM to shed light on the origin, transport, and biogeochemical transformation of OM in the subtropical karst reservoir ecosystems.

## 2. Materials and methods

### 2.1. Study Area

The DLD Reservoir, built in 1958, is located in a karst region of South China ( $23^{\circ}30'01''\sim 23^{\circ}40'08''$  N,  $108^{\circ}30'02''\sim 108^{\circ}36'04''$  E, Figure 1a), which is one of typical subtropical, groundwater-fed reservoirs in south China. The DLD reservoir has a surface area of approximately  $8.79 \times 10^6$  m<sup>2</sup> and a total storage capacity of  $1.51 \times 10^8$  m<sup>3</sup> and belongs to a junction of north–south and north–west faults [22,23]. The catchment of the DLD Reservoir is about 310 km<sup>2</sup> catchment, and about 99% of reservoir water is recharged by both two karst subterranean streams (Figure 1c). The study area is a subtropical monsoon humid climate area with a mean annual air temperature of 21.7 °C and mean annual precipitation of ~1294 mm, with most occurring from April to September. When the rainy season floods, smaller amounts of surface water occasionally pour into the DLD reservoir from Dongguan Reservoir (Figure 1c). The mean depth of the DLD reservoir is 11 m, and the maximum depth is 22.5 m [25]. The DLD reservoir is stratified from early April to late October (late spring, summer and early autumn) and mixed at other times (autumn, winter and most of spring) [23].

Around the reservoir, the main human activities are agriculture and tourism, with limited industry. At present, the reservoir is in a mild eutrophication state. The species of planktonic algae are abundant in the DLD reservoir. The phytoplankton species in the DLD reservoir include chlorophyta, diatom, Dinoflagellate, cryptomophyta and eukaryota. The number of phytoplankton in the water below the surface of the Dalong Reservoir decreased gradually, and the average density of phytoplankton cells in the 0.5 m, 2.5 m, 5 m and 10 m waters were  $974.0 \times 10^8$  L<sup>-1</sup>,  $2.965 \times 10^5$  L<sup>-1</sup>,  $154.6 \times 10^5$  L<sup>-1</sup> and  $3042 \times 10^5$  L<sup>-1</sup>, respectively. Chlorella is one of the dominant species in the DLD Reservoir. The average cell density of Chlorella in surface water is  $80.3 \times 10^5$  L<sup>-1</sup> [26]. Furthermore, some large submerged or emergent plants were found in the DLD reservoir around the reservoir and the hydro-fluctuation band at the tail of the reservoir (Figure 1c). The vertical distribution characteristics of bacterial abundance were as follows: surface layer > middle layer > bottom layer. The variation characteristics of bacterial productivity were that the bacterial productivity of surface water was significantly higher than that of middle and bottom water [27].

### 2.2. Sample Collection

A 52 cm-thick sediment core (SC3) was drilled using a gravity sediment sampler with a 58 mm internal diameter Perspex tube at the downstream part of the DLD reservoir in June 2015. In April 2016, the same type of gravity sediment sampler was used to collect the sediment cores of 82 cm (upstream SC1) and 84 cm (middle SC2), respectively (Figure 1c). The sediment cores were sub-sampled by 2 cm intervals in the field, stored in a cool box and taken back to the laboratory. In addition, the geochemical parameters such as total organic carbon (TOC), total organic nitrogen (TON), TOC/TON (C/N) ratios,  $\delta^{13}\text{C}$  of TOC, and  $\delta^{15}\text{N}$  of TON in sediment core samples were analyzed as described by [24] at the Chinese Academy of Agricultural Sciences. However, only 22 samples from three sediment core

samples at different depths (Figure 1c, Table S5) were used for the lipid biomarker analysis in this study.

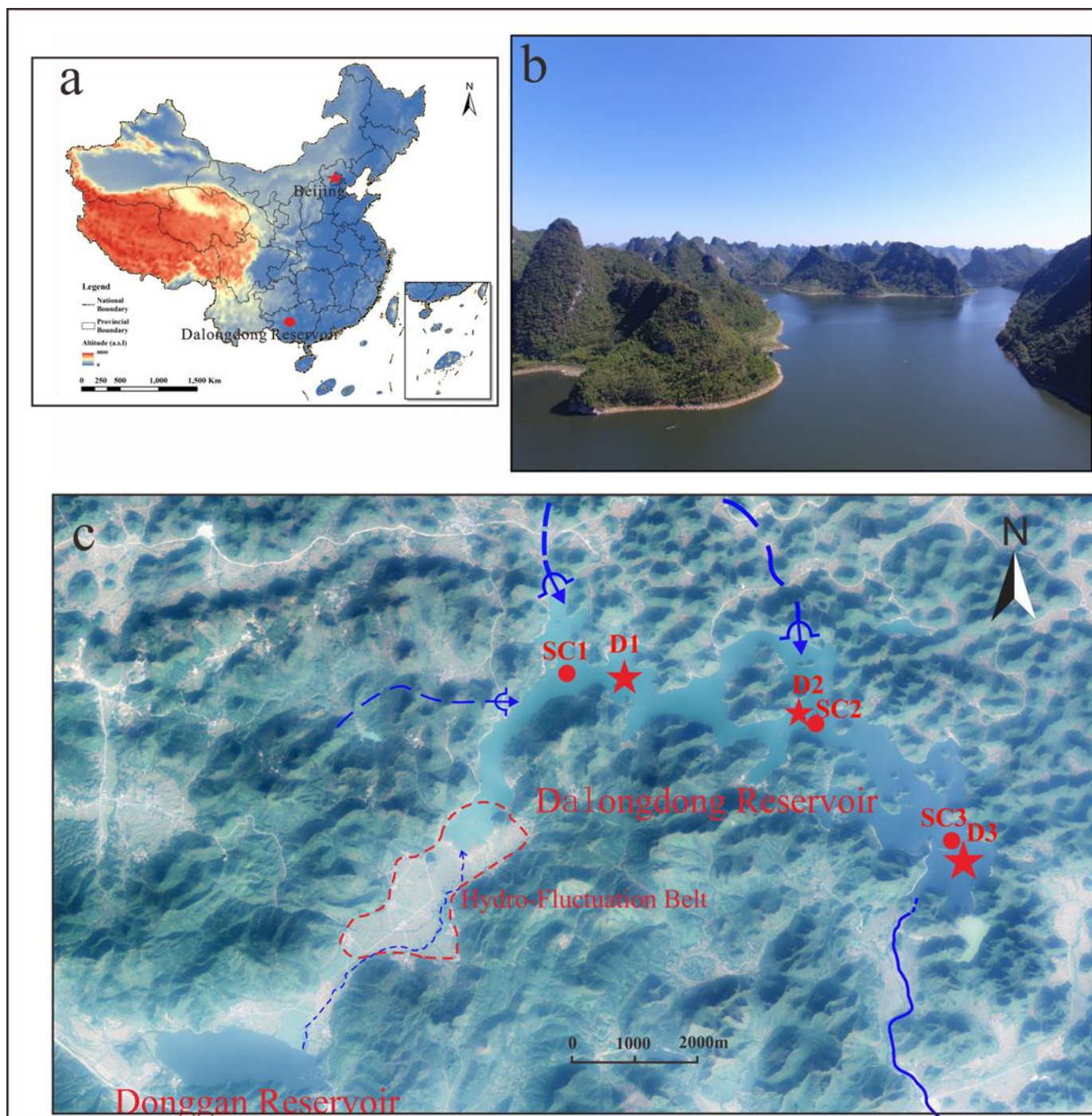


**Figure 1.** Location of the Dalongdong Reservoir, (a) A map of mainland China; (b) A landscape of Dalongdong Reservoir; and (c) A remote sensing map of the catchment area of DLD Reservoir. The red stars in panel (c) are DOM and POM sampling sites, and the red dots are sediment core sampling sites. (A blue, short-dashed line with an arrow and arc shows a karst subterranean stream. The thickness of the short blue line represents the flow of a karst subterranean stream. A long blue dashed line shows an ephemeral stream. A solid blue line shows a canal, which connected the reservoir by a headrace tunnel near the reservoir bottom).

The water samples were collected at 0.5 m (epilimnion) and 5 m (thermocline) below the water surface and bottom (hypolimnion) (0.5 m above the surface sediment) using a polyethylene tube connected to a peristaltic pump at D1, D2 and D3 site on 19 November 2019. The water was filtered onboard through a pre-extracted Whatman GF/F glass-fiber filter (pore size 0.7  $\mu\text{m}$ ). The volume of the filtered water is determined by the concentration of suspended particulates and is generally filtered 1–3 L. The filtrate water samples and the suspended material retained on the filter (coarse material) were immediately frozen at 4  $^{\circ}\text{C}$  for future lipid biomarker analysis and geochemical parameters at the laboratory. Furthermore, field environmental parameters, including water temperature (T,  $^{\circ}\text{C}$ ), pH, dissolved oxygen (DO, %), and redox potential (ORP, mV), were instantly measured in the field using a multi-parameter meter (YSI Pro Dss). The chlorophyll-a (Chla,  $\mu\text{g}\cdot\text{L}^{-1}$ ) was also measured in situ using UniLux fluorimeters (Chelsea Technologies, Inc., New York, NY, USA).

### 2.3. The Geochemical Parameters Analysis

Before laboratory analysis, the inorganic carbon in the sediment core samples and the POM samples were removed using 10% hydrochloric acid (HCl) and cleaned using ultrapure water until the water approached a pH of 7.0, and then the samples were dried in an oven at 55  $^{\circ}\text{C}$ . The POC and PON concentration and the  $\delta^{13}\text{C}$  and  $\delta^{15}\text{N}$  values were then determined by a Vario PYRO cube elemental analyzer (Vario PYRO cube, Isoprime, Hessen, Germany) coupled with an isotope ratio mass spectrometer (IRMS, ISOPRIME-100, Isoprime) at the Chinese Academy of Agricultural Sciences. The results are reported as delta notation ( $\delta^{13}\text{C}$ ,  $\delta^{15}\text{N}$ ) relative to Vienna PDB and atmospheric nitrogen, respectively. The standard deviations based on replicate measurements for  $\delta^{13}\text{C}$  and  $\delta^{15}\text{N}$  were both approximately 0.5‰. All the geochemical parameters analyses were carried out at the Environmental and Geochemical Analysis Laboratory of the Institute of Karst Geology, Chinese Academy of Geological Sciences.

### 2.4. Lipid Biomarker Analysis

The filtrate water samples were used to dissolved and particulate lipid biomarker analysis (DOOM and POM) as described by [28]. Briefly, 1.5 L filtered water was passed through a column (4 mL  $\text{min}^{-1}$ ) containing 5 g XAD-2 resin for the solid extraction of the lipids. Then, the lipids were retained on the XAD-2 resin, which was carried out by elution with two portions of methanol (50 mL each). The filters with the particulate matter ( $>0.7\ \mu\text{m}$ ) and sediment core samples were defrosted, and the first Soxhlet was extracted for 48 h with chloroform (9:1 *v/v*) to obtain the soluble fraction (free lipids), as described by [29,30]. The supernatants were concentrated to 1 mL by rotary evaporation at 40  $^{\circ}\text{C}$  after three centrifugations. The concentrated supernatants were purified and separated using solid-phase extraction (Rtx<sup>®</sup> ~5 mS, 30 m  $\times$  0.32 mm  $\times$  0.25  $\mu\text{m}$  DB5 column) and n-hexane, and then the eluent with n-alkanes was concentrated to 1 mL. Compounds were quantified using total ion current (TIC) peak area and converted to compound mass using calibration curves of external standards. The GC conditions were as follows: For fatty acids, the temperature was programmed from 60  $^{\circ}\text{C}$  to 150  $^{\circ}\text{C}$  at 40  $^{\circ}\text{C}/\text{min}$ . Then, the temperature was increased to 240  $^{\circ}\text{C}$  (held for 15 min) at 3  $^{\circ}\text{C}/\text{min}$ . For n-alkanes, the temperature was raised from 70  $^{\circ}\text{C}$  (held for 1 min) to 140  $^{\circ}\text{C}$  at 10  $^{\circ}\text{C}/\text{min}$ , and then at 3  $^{\circ}\text{C}/\text{min}$  to 310  $^{\circ}\text{C}$  (held for 15 min). All lipid biomarker analyses were carried out at the Environmental and Geochemical Analysis Laboratory of the Institute of the Third marine Institute, ministry of Natural Resources. Detailed methods of extracting lipid biomarkers from sediment and water are shown in the attachment.

## 3. Results

### 3.1. Physicochemical Properties, Carbon and Nitrogen Isotopes

The DLD reservoir is stratified from early April to late October (late spring, summer and early autumn) and mixed at other times (autumn, winter and most of spring) [23].

The maximum temperature difference between the upper and lower layers reached is 10 °C during the stratification period [22]. The basic physicochemical properties and isotopic results are shown in Table 1. We can notice that the water temperature (T) ranged from 19.0 °C to 21.6 °C, with a mean value of  $20.8 \pm 0.95\%$ , indicating that there is no obvious stratification of water temperature. However, the basic physicochemical properties and isotopic results still show obvious stratification. The pH, dissolved oxygen (DO), redox potential (ORP), and chlorophyll a (Chla) have high values in epilimnion (0.5 m) and low values in the hypolimnion, indicating that the biomass of subaquatic phototrophs was high in the epilimnion and low in the hypolimnion. Additionally, it suggests that the epilimnion is an oxidizing environment while the hypolimnion is a reducing environment. The TOC and DOC concentrations increase with water depth, ranging from 1.61 to 2.51 mg/L, with a mean value of 1.95 mg/L and from 0.84 to 2.41 mg/L with a mean value of 1.54 mg/L, respectively. In contrast, the POC concentrations decrease with water depth, ranging from 0.05 to 2.41 mg/L, with a mean value of 0.27 mg/L. In addition, the  $\delta^{13}\text{C}_{\text{POC}}$  in epilimnion ( $-35.07 \pm 0.62\%$ ) were significantly obviously more negative than hypolimnion ( $-31.45 \pm 1.30\%$ ). In contrast, the  $\delta^{15}\text{N}_{\text{PON}}$  in epilimnion ( $9.32 \pm 1.16\%$ ) were little positive than hypolimnion ( $8.42 \pm 1.30\%$ ). The average molar C/N values were  $6.10 \pm 0.10$ ,  $6.30 \pm 0.20$  and  $7.27 \pm 0.25$  at the epilimnion, thermocline and hypolimnion, respectively, showing little difference between them. The stratification of the basic physicochemical properties and isotopic reflected that when we collected the water samples (19 November 2019), the DLD reservoir was not fully mixed; it was in the transition period from the stratification period to the mixing period.

**Table 1.** The basic hydrochemical, elemental (C/N ratios), and isotope ratios ( $\delta^{13}\text{C}$  and  $\delta^{15}\text{N}$ ) of water.

Site	Depth (m)	T (°C)	PH	DO (%)	ORP (mV)	Chla ( $\mu\text{g/L}$ )	TOC (mg/L)	DOC (mg/L)	POC (mg/L)	$\delta^{13}\text{C}_{\text{POC}}$ (‰)	$\delta^{15}\text{N}_{\text{PON}}$ (‰)	C/N
D1-1	0.5	20.8	8.01	83.2	244.8	11.11	1.61	0.84	0.65	-35.06	10.56	6.00
D1-2	5.0	21.4	8.01	81.5	216.9	10.48	2.43	1.98	0.27	-34.28	11.05	6.10
D1-3	7.5	21.6	7.98	78.7	176.9	9.25	2.51	2.41	0.05	-31.21	8.60	7.00
D2-1	0.5	21.3	7.9	70.1	216.4	7.765	1.76	1.01	0.67	-35.69	8.27	6.10
D2-2	5.0	21.4	7.89	70.7	219.7	8.512	1.87	1.58	0.24	-34.14	9.61	6.30
D2-3	11.5	20.3	7.14	18.9	-80.5	5.43	1.95	1.87	0.05	-32.85	8.69	7.50
D3-1	0.5	19.5	7.82	78.4	154.3	6.502	1.73	0.99	0.69	-34.45	9.13	6.20
D3-2	5.0	21.5	7.81	71.1	163.5	5.992	1.82	1.48	0.30	-33.34	7.84	6.50
D3-3	13	19.0	7.15	18.0	-79.8	1.954	1.85	1.69	0.06	-30.28	7.98	7.30
Mean	-	20.8	7.75	63.40	136.91	7.44	1.95	1.54	0.33	-33.48	9.08	6.56
SD	-	0.95	0.35	25.93	126.52	2.84	0.31	0.52	0.27	1.78	1.13	0.57

### 3.2. Contents and Composition Characteristics of n-Alkanes and Fatty Acids

The n-alkane concentrations in the POM samples ranged from 0.19  $\mu\text{g/L}$  to 0.80  $\mu\text{g/L}$  (mean =  $0.39 \pm 0.21 \mu\text{g/L}$ ), which is higher than that in the DOM samples (ranged from 0.16  $\mu\text{g/L}$  to 0.33  $\mu\text{g/L}$ , mean =  $0.25 \pm 0.05 \mu\text{g/L}$ ) (Table S1). The n-alkane concentrations in the SCOM samples ranged from 3.94  $\mu\text{g/g}$  to 9.39  $\text{ng/g}$  (mean =  $6.52 \pm 1.54 \text{ng/g}$ ) (Tables S2 and S3). The carbon numbers of the n-alkanes in the POM samples and DOM samples are similar, with homologues ranging from  $\text{C}_{16}$  to  $\text{C}_{34}$  (Table S1, Figure 2). Slightly different from the previous two, the range of the n-alkanes in most SCOM samples was  $\text{C}_{15}$ – $\text{C}_{33}$ . It should be noted that the relative concentrations of the individual components of different types of OM differ markedly (Figure 2). Additionally, the C19 and C20 isoprenoids, pristane (Pr) and phytane (Ph), respectively, are believed to be end products resulting from the degradation of chlorophyll a's phytol side chain in aquatic environments. However, whether Pr or Ph is formed depends on the environmental conditions, particularly its oxygen level. Although other sources are possible for these isoprenoids, the ratio of Pr/Ph is commonly used as an indicator of the environment's oxygenation [28]. The Pr/Ph ratios for the SCOM samples were 0.18–1.74 (mean 1.01) (Tables S2 and S3, Figure 2c). most

samples from core 3 and the upper samples from cores 1 and 2 had Pr/Ph values greater than 1, indicating reducing conditions at the sampling site. The fluctuations in Pr/Ph appear to be linked to sedimentary processes influenced by environmental differences at the locations where the samples were collected.

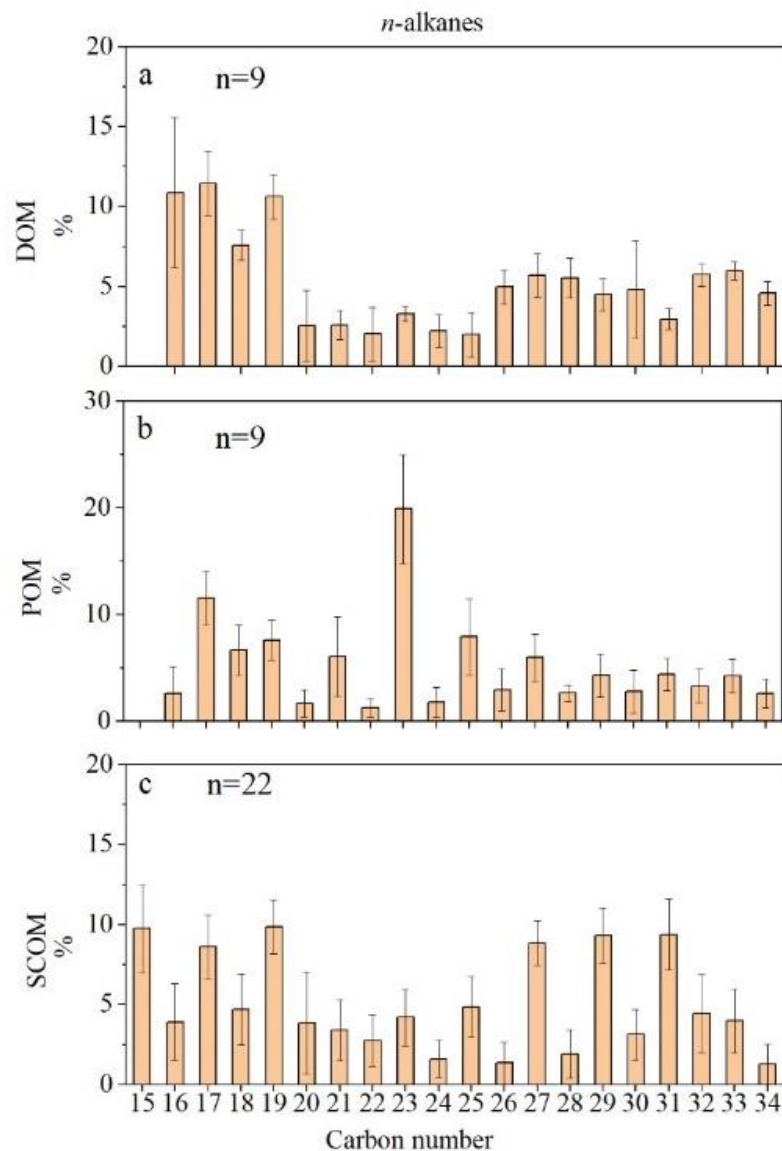


**Figure 2.** Histograms of the distributions of n-alkane for the  $n$  species from the three types of OM: (a) DOM, (b) POM, and (c) SCOM. Bars represent 1 standard deviation.

The total fatty acid (TFA) concentrations were 1.75–21.83  $\mu\text{g}/\text{L}$  (mean  $5.31 \pm 6.37 \mu\text{g}/\text{L}$ ) in the DOM samples, which were obviously lower than that in the POM samples (ranged from 14.43 ng/L to 42.81  $\mu\text{g}/\text{L}$ , mean =  $24.84 \pm 8.69 \mu\text{g}/\text{L}$ ). The TFA concentrations in the SCOM samples ranged from 0.83 ng/g to 48.11 ng/g (mean =  $14.93 \pm 11.78 \text{ ng}/\text{g}$ ) (Tables S3 and S4). Here, fatty acids were divided into saturated fatty acids (SFA) and unsaturated fatty acids (UFA). UFA included monounsaturated fatty acids (MUFA) and polyunsaturated fatty acids (PUFA). The fatty acids in all samples were mainly composed of SFA. The percentage of SFA in the SCOM samples was the highest of the three types, with samples ranging from 87.71% to 97.96% with an average of  $95.17 \pm 2.71\%$ . The percentage of SFA ranged from 27.97% to 79.85% with an average of  $59.68 \pm 15.00\%$  in the DOM samples and ranged from 50.50% to 72.50% with an average of  $57.25 \pm 7.33\%$  in the POM samples (Figure 3).

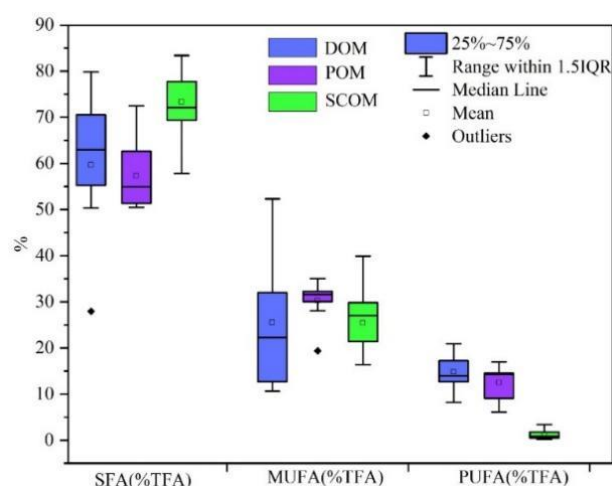


Figure 3. Box plots of the fatty acid compositions.

## 4. Discussion

### 4.1. Lipid Biomarker Indicators of DOM, POM, and SCOM Sources

Lipid biomarker analyses have been shown to be an effective tool for examining complex sources of organic matter characteristics in aquatic systems. The aliphatic hydrocarbon fractions were mainly composed of autochthonous-derived short-chain  $n$ -C<sub>16</sub> to  $n$ -C<sub>19</sub> or  $n$ -C<sub>15</sub> to  $n$ -C<sub>19</sub> in the DOM and SCOM samples (Figure 2a,c), especially the odd-numbered  $n$ -alkanes  $n$ -C<sub>17</sub> and  $n$ -C<sub>19</sub>, are remarkable, indicating that these two types of samples mostly consisted of algae. middle-chain  $n$ -C<sub>23</sub> dominates in the POM samples, indicating that the POM samples primarily come from submerged and floating aquatic plants (Figure 2b). Long-chain  $n$ -C<sub>27</sub> to  $n$ -C<sub>34</sub> derived from allochthonous were also observed in SCOM samples, indicating that the SCOM samples in the DLD reservoir also have terrestrial sources [5].

In addition, C16:0 (Palmitic acid) was the most abundant compound in all samples, which accounted for an average of 35.0% of the TFA. The mUFA usually represents the activity of diatom growth in aquatic systems and has been used to evaluate the autochthonous production capacity [9,31]. We should be concerned that C16:1 $\omega$  (Palmitoleic acid) was observed in samples, which was the major mUFA and considered an indicator of autochthonous production (Figure 4a). The percentage of mUFA in DOM samples is greater than in POM samples (Figure 3). However, the POM sample at P2-3 contained the most abundant C16:1 $\omega$  (48.81 mg/L). The presence of C16:1 $\omega$  indicated that the photosynthesis of phytoplankton was intense in the DLD reservoir [9,31].

In order to more accurately analyze the source of OM and quantify the proportion of different sources, the  $n$ -alkane proxy TAR<sub>HC</sub> and  $P_{aq}$  have been calculated. The  $P_{aq}$  can be used to distinguish the relative proportions of terrigenous plants, emergent aquatic plants and submerged aquatic plant inputs [32], and the TAR<sub>HC</sub> was used to assess the relative contributions of autochthonous (low TAR<sub>HC</sub> value) and allochthonous (high TAR<sub>HC</sub> value) hydrocarbons in aquatic environments [20]. The attached Tables S1–S3 list the calculated  $n$ -alkane indices values for all samples. The box plot of each indicator is displayed in Figure 5. The TAR<sub>HC</sub> values for all samples ranged from 0.00  $\mu$ g/L to 1.66  $\mu$ g/L, with a mean value of  $0.55 \pm 0.39$ —most of which are in the eigenvalue range of the aquatic plants control (Figure 5a, TAR<sub>HC</sub> < 1) [5]. The  $P_{aq}$  values for all samples ranged from 0.00 to 1.00, with a mean value of  $0.60 \pm 0.23$ ; most of them are also in the eigenvalue range of aquatic plants control (Figure 5b,  $P_{aq}$  < 0.25). These two indicators strongly reflect the OM of DLD reservoir dominance to aquatic plants again. In summary, autochthonous (algal or plankton) sources are the major sources in the DOM, POM, and SCOM to the karst reservoir ecosystems, but the relative contribution of autochthonous sources in POM was higher than that in DOM and SCOM (Figure 5a,b).

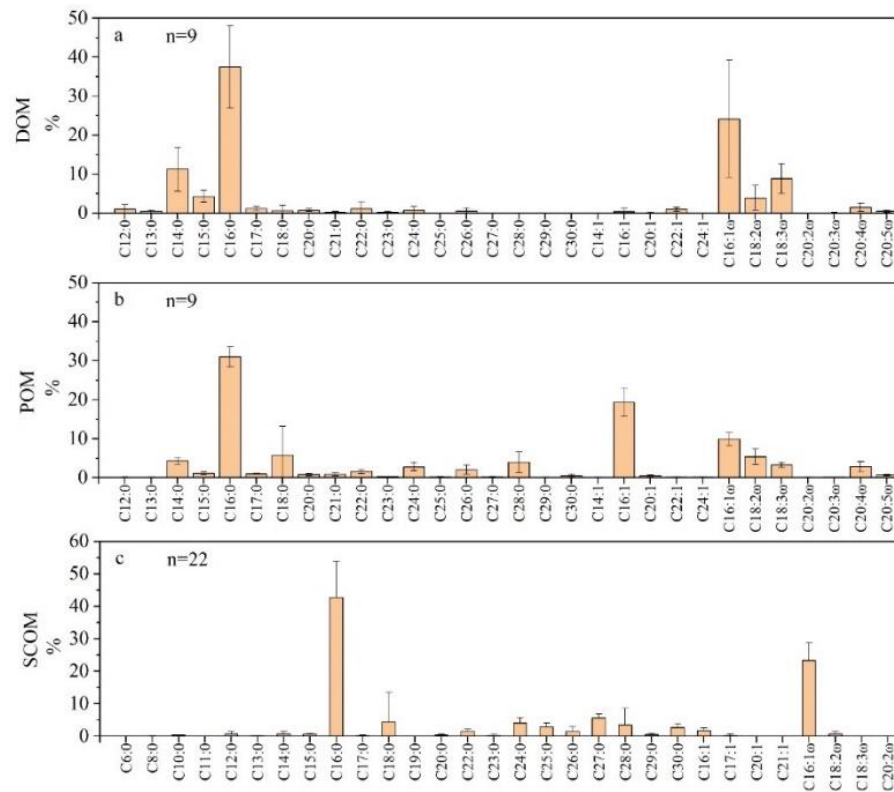


**Figure 4.** Histograms of the distributions of fatty acids for *n* species from the three types of OM: (a) DOM, (b) POM, and (c) SCOM. Bars represent a standard deviation of 1.

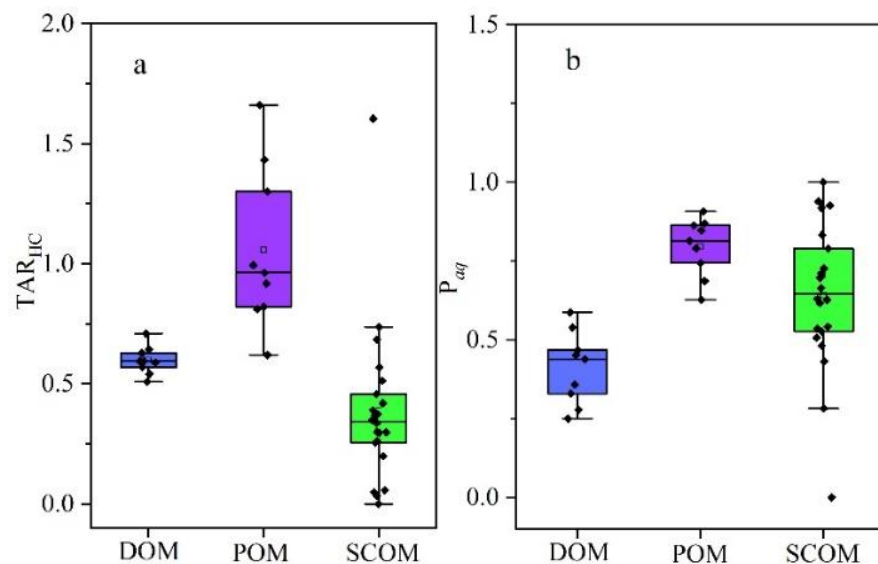


**Figure 5.** A box plot of the n-alkane indices TAR<sub>HC</sub> (a) and P<sub>aq</sub> (b). (The upper cross, lower cross, square, lower edge, upper edge, bars, black line in or outside the boxes refer to max and min values, 25th and 75th, 5th and 95th, and <5th and >95th percentiles of all data, respectively).

We created three triangular diagrams, each based on the concentration of different compounds, to indicate their respective sources: n-alkanes. In the three triangular diagrams, we used the C15 + C17 + C19 n-alkanes to represent OM of bacterial origin and C21 + C23 + C25 n-alkanes to represent the OM from aquatic plants, while the C27 + C29 + C31 n-alkanes to represent the terrigenous OM. It is seen in Figure 6 that the bacteria were the main contributors to n-alkanes, contributing around 50% to the n-alkanes

of DOM, and aquatic plants OM contributed a lower 25% to the n-alkanes of DOM. However, in POM, terrestrial OM and aquatic plant OM were primary contributors to n-alkanes, with bacteria playing a minor role. Similarly, in SCOM, bacterial-originated OM remained the main contributor (over 50%) to n-alkane content, while terrestrial OM accounted for less than 25%, similar to its contribution in POM.

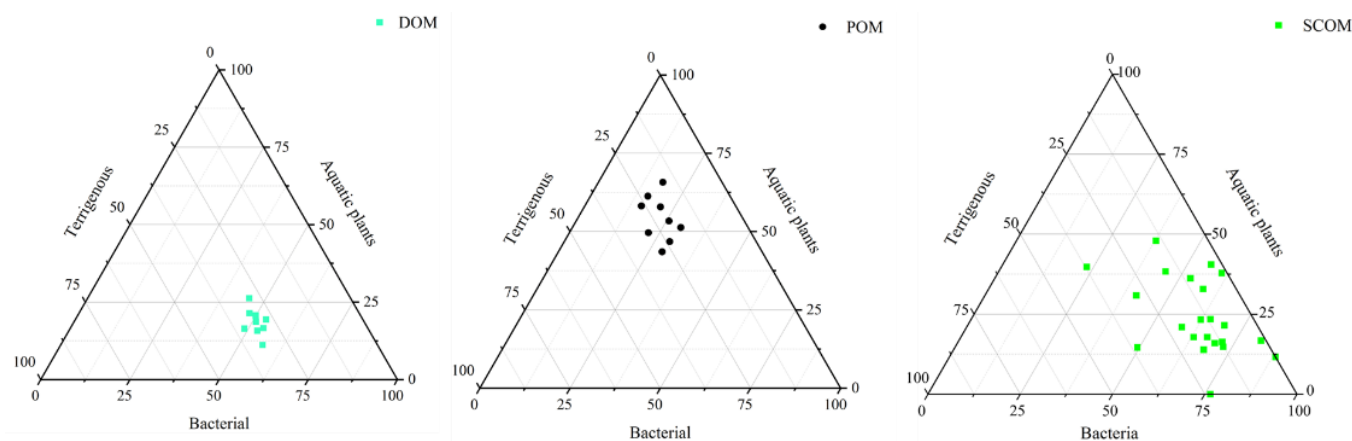


**Figure 6.** Contribution rates of three sources in n-alkanes from DOM, POM, and SCOM samples.

#### 4.2. Microbial Activity Inferred from the Lipid Biomarker Data

As shown in Figure 7, the odd-over-even predominance (OEP) value and ratios of C16:1/C16:0 in POM were obviously higher than those in DOM. The mean OEP values in DOM and POM were 1.08 and 2.87, respectively, and the mean ratios of C16:1/C16:0 were 0.01 and 0.63, respectively. The primary reason for this phenomenon is the initial development of OEP as a method to identify petroleum sources (distribution of n-paraffins as an indicator for source beds). Subsequently, OEP has been extensively utilized in studies of various environmental settings, including soil and sediments, to determine the origins of n-alkanes and evaluate their level of degradation (Postglacial climate-change record in biomarker lipid compositions of the Hani peat sequence, Northeastern China). Elevated values for OEP indicate that the n-alkanes are derived from plant waxes and signify well-preserved biomarker signals (diagenesis of free and bound lipids in terrestrial detritus deposited in a lacustrine sediment) [5,9,19]. Conversely, lower values typically indicate alternative sources of n-alkanes, such as microbial origins or a significant level of degradation (diagenesis of free and bound lipids in terrestrial detritus deposited in lacustrine sediment). In addition, the significance of the C16:1/C16:0 ratio in lipid biogeochemistry is that it can provide insights into the degree of degradation or alteration that the lipid molecules have undergone. When degradation processes, such as oxidation or microbial degradation, become important, they can affect the composition of fatty acids in a sample. Specifically, the ratio tends to decrease when degradation processes are more active. The rationale behind this is as follows: unsaturated fatty acids contain one or more double bonds, while saturated fatty acids have no double bonds [5]. Unsaturated fatty acids (C16:1) exhibit a higher susceptibility to degradation compared to saturated fatty acids (C16:0), owing to their increased chemical reactivity resulting from the presence of double bonds. Consequently, as unsaturated fatty acids degrade, the relative proportion of saturated fatty acids in the sample (C16:0) increases while that of unsaturated ones (C16:1) decreases, leading to a decline in the C16:1/C16:0 ratio [29]. In essence, the data in Figure 7 and the accompanying text suggest that there are notable differences in organic matter composition and microbial activity between DOM and POM, with POM having higher OEP values and C16:1/C16:0 ratios, indicating potentially lower microbial degradation in POM compared to DOM. This information is valuable for understanding the dynamics of organic matter in the studied environment.

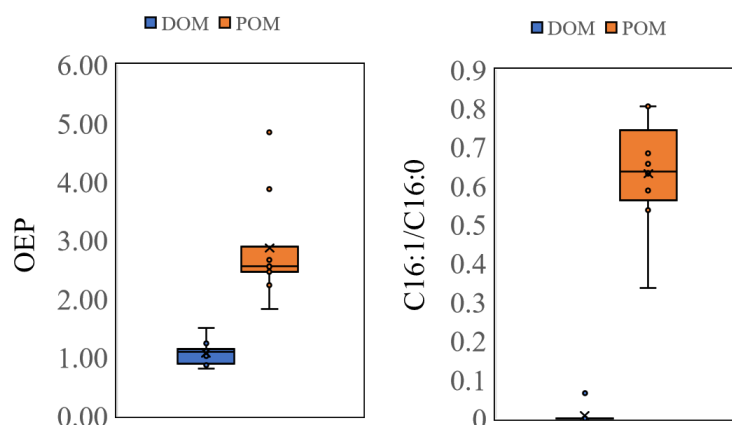


**Figure 7.** Distribution values of OEP and C16:1/C16:0 in DOM and POM. (The upper cross, lower cross, square, lower edge, upper edge, bars, black line in or outside the boxes refer to max and min values, 25th and 75th, 5th and 95th, and <5th and >95th percentiles of all data, respectively).

For further study, factors affecting the sources and distributions of n-alkanes in DOM and POM, related hydrochemical parameters were discussed in this study. It can be seen in Figure 8 that water depth positively correlated with DOC ( $p < 0.05$ ),  $\delta^{13}\text{C}_{\text{POC}}$  ( $p < 0.01$ ), and  $\text{TAR}_{\text{HC}}$  in POM ( $p < 0.01$ ) but negatively correlated with POC ( $p < 0.05$ ), and L/H in POM ( $p < 0.05$ ), indicating that DOC concentrations in the DLD Reservoir increased with water depth, while POC concentrations decreased with water depth. In addition, DO concentrations positively correlated with Chla ( $p < 0.01$ ),  $\Sigma$ n-alkane concentrations in DOM ( $p < 0.05$ ), L/H in POM ( $p < 0.01$ ), but negatively correlated with  $\text{TAR}_{\text{HC}}$  in POM ( $p < 0.01$ ), and  $\text{CPI}_{\text{HC}}$  in POM ( $p < 0.01$ ). Eh positively correlated with Chla ( $p < 0.01$ ), OEP in DOM ( $p < 0.01$ ), and  $\text{CPI}_{\text{HC}}$  in DOM ( $p < 0.01$ ). It can be concluded that the transformation of n-alkanes in DOM was obviously influenced by Eh, while the degree of higher plant degradation in POM was obviously influenced by the concentration of DO in the DLD Reservoir.

The conclusion that the transformation of n-alkanes in dissolved organic matter (DOM) is influenced by the Eh, while the degradation of higher plants in particulate organic matter (POM) is influenced by the concentration of dissolved oxygen (DO) in the DLD Reservoir, can be explained in the following manner: (1) DO is a critical parameter in aquatic ecosystems as it directly affects the respiratory activities of organisms, including microorganisms responsible for organic matter degradation. POM primarily consists of larger organic particles, such as plant debris and detritus. Higher plant degradation refers to the breakdown and decomposition of organic matter derived from aquatic macrophytes or emergent plants. When DO concentrations are high, aerobic microorganisms can thrive and efficiently decompose the higher plant material in POM through aerobic respiration, leading to its degradation. However, in conditions of low DO concentrations, the decomposition of higher plant material may slow down or be inhibited, as anaerobic microorganisms may dominate, and anaerobic processes become more prevalent [5,6]. (2) Eh is a measure of the redox state of a system, indicating whether it is oxidizing or reducing. In aquatic environments, Eh plays a crucial role in determining the availability of electron acceptors and donors, which can influence biogeochemical processes. The transformation of n-alkanes in DOM refers to the breakdown and alteration of these hydrocarbons, which are common constituents of organic matter. The presence of electron acceptors or oxidizing conditions (higher Eh values) in the water can promote the microbial degradation of n-alkanes, leading to their transformation into simpler compounds. Conversely, under reducing conditions (lower Eh values), the availability of electron acceptors may be limited, inhibiting the microbial degradation of n-alkanes in DOM [31,32]. In summary, the observed correlations suggest that the redox conditions represented by Eh influence the transformation of n-alkanes in DOM, while the concentration of DO impacts the degradation of higher plants

in POM. These relationships highlight the important role of redox conditions and dissolved oxygen availability in shaping the fate and dynamics of organic matter components in the DLD Reservoir ecosystem. The understanding of these factors can provide valuable insights into the carbon cycling and overall ecological functioning of the reservoir. However, it is essential to acknowledge that these are observational correlations, and additional experiments or modeling studies would be required to establish direct cause-and-effect relationships between Eh, DO, and organic matter transformations in the DLD Reservoir.

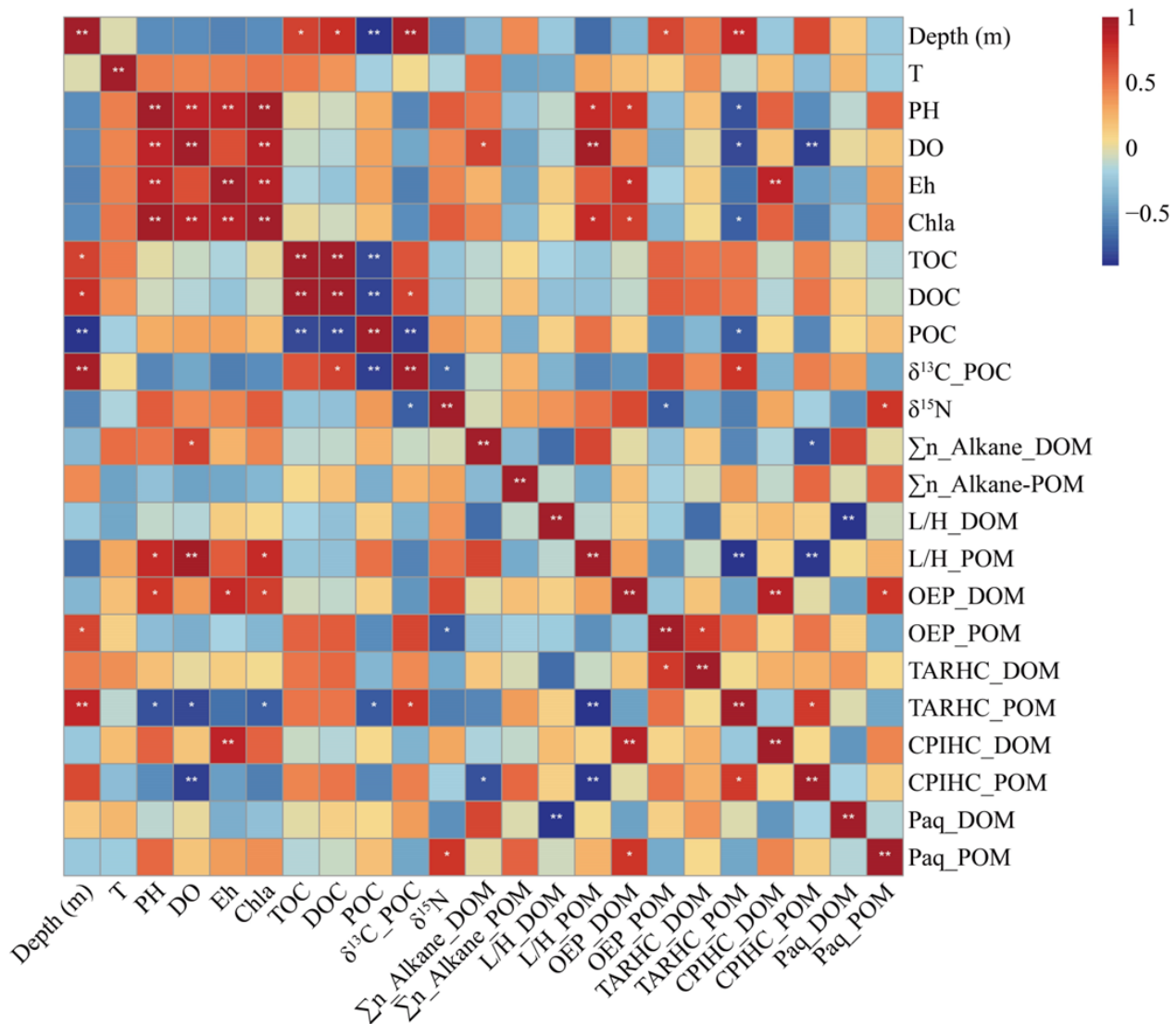


**Figure 8.** Pearson's correlation coefficients for the relationships between n-alkanes indices and the related hydrochemical parameters. (convention for symbols indicating statistical significance \*:  $p \leq 0.05$ ; \*\*:  $p \leq 0.01$ ).

#### 4.3. Comparison of Lipids Found in the DOM and POM Samples

The concentrations of lipid biomarkers (n-alkanes and fatty acids) in both the DOM and POM samples exhibited similar spatial variations (Figure 9), suggesting that similar processes influenced the concentrations of lipid biomarkers in both the DOM and POM samples. However, the contributions of aquatic plants OM to the total OM concentrations were higher for the POM samples than for the DOM samples, as indicated by the contribution of mid-chain n-alkyl lipids being higher for the POM than for the DOM samples (Figure 5). This is evident from the triangular diagrams depicted in Figure 6. In line with this, the  $\delta^{13}\text{C}_{\text{POC}}$  values of OM and  $\delta^{13}\text{C}_{\text{PON}}$  in the POM samples closely matched those

of autochthonous OM [24]. Previous studies have proposed that autochthonous organic carbon originating from aquatic phytoplankton is relatively labile and susceptible to microbial utilization during and after sedimentation, whereas terrestrial OM is comparatively refractory and poses challenges for microbial degradation (lipid biomarkers in suspended particulate matter and surface sediments in the Pearl River Estuary, a subtropical estuary in southern China). As can be seen from Figure 6, the contribution of macrophyte OM in POM and SCOM was obviously higher than those in DOM, similar to terrestrial OM, which is also comparatively refractory and poses challenges for microbial degradation compared to autochthonous organic carbon originating from aquatic phytoplankton.

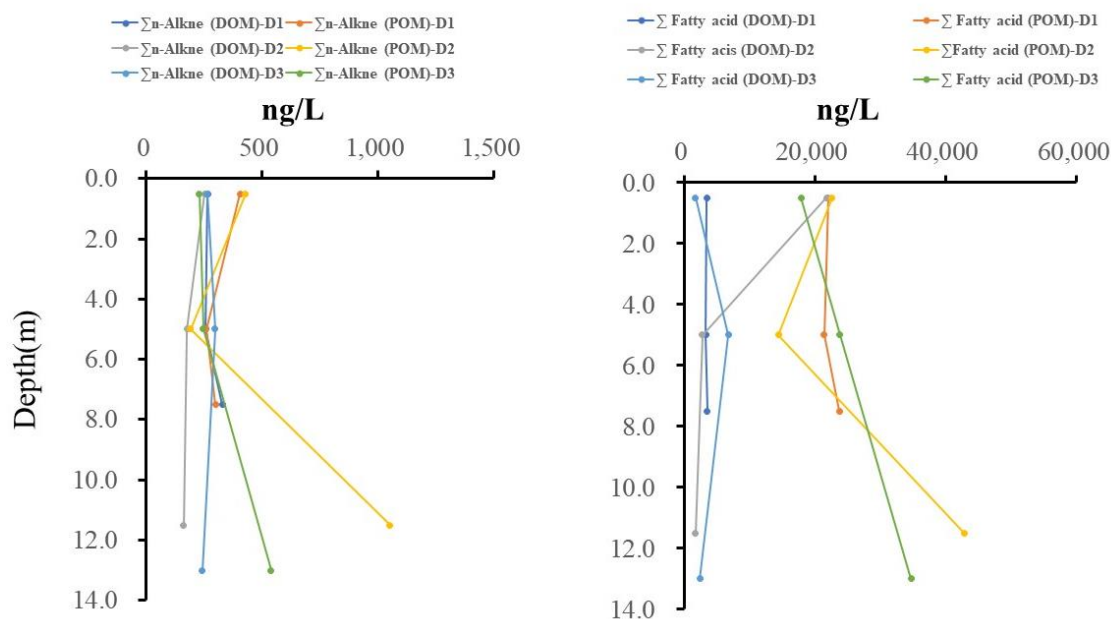


**Figure 9.** Total n-alkanes and fatty acids concentrations in the DOM and POM along different water depths in the DLD Reservoir.

## 5. Conclusions and Research Perspectives

- (1) The presence and distribution patterns of lipid biomarkers (including fatty acids) suggested that phytoplankton and bacteria were the primary contributors of OM in both the DOM and SCOM, while inputs from terrestrial vascular plants and aquatic plants were found to be the main contributors in POM. This conclusion suggests that phytoplankton and bacteria are the primary contributors of organic matter in both DOM and SCOM. At the same time, inputs from terrestrial vascular plants and aquatic plants are the main contributors to particulate organic matter (POM). Phytoplankton and bacteria are crucial components of marine and freshwater ecosystems, and they perform photosynthesis, converting atmospheric carbon dioxide into organic matter. Therefore, their dominance as primary contributors to OM in DOM and SCOM indicates their potential role in sequestering carbon from the atmosphere and contributing to carbon burial in sediments, which could act as a carbon sink, mitigating the impacts of climate change. On the other hand, the significant contribution of terrestrial and aquatic plant-derived OM to POM suggests that organic matter from vegetation plays a critical role in the carbon cycle. If these plants grow in large quantities, they can sequester carbon from the atmosphere through photosynthesis. However, their contribution to POM also means that this carbon can be more readily released back into the environment through degradation processes. Thus, the balance between carbon sequestration by plants and the susceptibility of plant-derived OM to degradation is vital in the context of global climate change.
- (2) The distinct degradation patterns of lipid biomarkers may have led to the observed variations in lipid composition and distribution between the DOM and POM samples,

resulting in a greater contribution of terrigenous and macrophytes lipids to POM compared to DOM. This observation implies that terrigenous and macrophyte OM are relatively more resistant to degradation than aquatic phytoplankton origin. This observation points to variations in lipid composition and distribution between DOM and POM, with terrigenous and macrophyte OM being relatively more resistant to degradation than OM derived from aquatic phytoplankton. The resistance of terrigenous and macrophyte OM to degradation implies that a portion of the carbon stored in these sources may persist in the environment for more extended periods before being released as CO<sub>2</sub>. In contrast, OM derived from aquatic phytoplankton is more susceptible to degradation, leading to a faster return of carbon to the atmosphere. These conclusions collectively highlight the intricate dynamics of organic matter in different components of aquatic ecosystems and its potential impact on the global carbon cycle. Understanding the sources, transformations, and degradation patterns of organic matter are essential for predicting and modeling carbon fluxes, carbon sequestration potential, and overall climate change dynamics at both regional and global scales.

**Supplementary Materials:** The following supporting information can be downloaded at: <https://www.mdpi.com/article/10.3390/w15183255/s1>, Table S1: n-alkane of POM and DOM samples (ng/L); Table S2: n-alkanes of sediment core 1 and sediment core 2 (μg/g); Table S3: n-alkanes of sediment core 1 and sediment core 3 (μg/g); Table S4: Fatty acids of POM and DOM samples (μg/L); Table S5: 22 sediment cores for depth of sampling and location coordinates. Figure S1: Spectra of C15–C34 n-alkanes in alkane mixing standard and D3 sediment samples; Figure S2: Spectrum and integral results of alkanes (D3-1A) before and after purification of D3 deposits by 10% silver nitrate silica gel (D3-1); Figure S3: Coincidence spectra of C12–C24 fatty acids in fatty acid components of D3 sediment and fatty acid mixing standard.

**Author Contributions:** J.L.: field sampling, laboratory test, data processing, software, writing—original draft, writing—review and editing; J.P. and T.Z.: methodology, field sampling, supervision; X.T.: data processing, review and editing; Y.X.: field sampling, laboratory test; Q.X.: writing—review and editing. All authors have read and agreed to the published version of the manuscript.

**Funding:** This study was supported by the National Natural Science Foundation of China (NO. 41977166, 41907172), the Guangxi Natural Science Foundation (NO. GuikeAB21196050, NO. 2020GXNS-FAA297266), the Natural Science Foundation of Chongqing, China (NO. CSTB2022NSCQ-LZX0022, NO. CSTB2022NSCQ-MSX0619) and China Geological Survey (NO.DD20230547).

**Data Availability Statement:** In addition to the attached data, the data used in this study will not be made publicly available.

**Conflicts of Interest:** The authors declare no competing financial interest.

## References

1. Lam, B.; Baer, A.; Alae, m.; Lefebvre, B.; Moser, A.; Williams, A.; Simpson, A.J. major structural components in freshwater dissolved organic matter. *Environ. Sci. Technol.* **2007**, *41*, 8240–8247. [[CrossRef](#)]
2. Battin, T.J.; Luyssaert, S.; Kaplan, L.A.; Aufdenkampe, A.K.; Richter, A.; Tranvik, L.J. The boundless carbon cycle. *Nat. Geosci.* **2009**, *2*, 598–600. [[CrossRef](#)]
3. Poulter, B.; Frank, D.; Ciais, P.; myneni, R.B.; Andela, N.; Bi, J.; Broquet, G.; Canadell, J.G.; Chevallier, F.; Liu, Y.Y.; et al. Contribution of semi-arid ecosystems to interannual variability of the global carbon cycle. *Nature* **2014**, *509*, 600–603. [[CrossRef](#)]
4. Vonk, J.E.; van Dongen, B.E.; Gustafsson, Ö. Lipid biomarker investigation of the origin and diagenetic state of sub-arctic terrestrial organic matter presently exported into the northern Bothnian Bay. *Mar. Chem.* **2008**, *112*, 1–10. [[CrossRef](#)]
5. Derrien, m.; Yang, L.; Hur, J. Lipid biomarkers and spectroscopic indices for identifying organic matter sources in aquatic environments: A review. *Water Res.* **2017**, *112*, 58–71. [[CrossRef](#)]
6. Meng, L.; Zhao, Z.; Lu, L.; Zhou, J.; Luo, D.; Fan, R.; Li, S.; Jiang, Q.; Huang, T.; Yang, H.; et al. Source identification of particulate organic carbon using stable isotopes and n-alkanes: modeling and application. *Water Res.* **2021**, *197*, 117083. [[CrossRef](#)]
7. Liu, Z.; Dreybrodt, W.; Wang, H. A new direction in effective accounting for the atmospheric CO<sub>2</sub> budget: Considering the combined action of carbonate dissolution, the global water cycle and photosynthetic uptake of DIC by aquatic organisms. *Earth-Sci. Rev.* **2010**, *99*, 162–172. [[CrossRef](#)]

8. Liu, H.; Chen, B.; Yang, R.; Yan, Z. Carbon sequestration and decreased CO<sub>2</sub> emission caused by terrestrial aquatic photosynthesis: Insights from diel hydrochemical variations in an epikarst spring and two spring-fed ponds in different seasons. *Appl. Geochem. J. Int. Assoc. Geochem. Cosmochem.* **2015**, *63*, 248–260.
9. Yang, m.; Liu, Z.; Sun, H.; Rui, Y.; Bo, C. Organic carbon source tracing and DIC fertilization effect in the Pearl River: Insights from lipid biomarker and geochemical analysis. *Appl. Geochem.* **2016**, *73*, 132–141. [[CrossRef](#)]
10. Liu, Z.; macpherson, G.L.; Groves, C.; martin, J.B.; Yuan, D.; Zeng, S. Large and active CO<sub>2</sub> uptake by coupled carbonate weathering. *Earth Sci. Rev.* **2018**, *182*, 42–49. [[CrossRef](#)]
11. Henderson, R.K.; Baker, A.; murphy, K.R.; Hambly, A.; Stuetz, R.M.; Khan, S.J. Fluorescence as a potential monitoring tool for recycled water systems: A review. *Water Res.* **2009**, *43*, 863–881. [[CrossRef](#)] [[PubMed](#)]
12. Cloern, J.E.; Harris, C.D. Stable carbon and nitrogen isotope composition of aquatic and terrestrial plants of the San Francisco Bay estuarine system. *Limnol. Oceanogr.* **2002**, *47*, 713–729. [[CrossRef](#)]
13. Sojiniu, S.O.; Sonibare, O.O.; Ekundayo, O.; Zeng, E.Y. Assessing anthropogenic contamination in surface sediments of Niger Delta, Nigeria with fecal sterols and n-alkanes as indicators. *Sci. Total Environ.* **2012**, *441*, 89–96. [[CrossRef](#)] [[PubMed](#)]
14. Zhang, S.; Li, S.; Dong, H.; Zhao, Q.; Lu, X.; Shi, J. An analysis of organic matter sources for surface sediments in the central South Yellow Sea, China: Evidence based on macroelements and n-alkanes. *Mar. Pollut. Bull.* **2014**, *88*, 389–397. [[CrossRef](#)] [[PubMed](#)]
15. Blyth, A.J.; Asrat, A.; Baker, A.; Gulliver, P.; Leng, m.J.; Genty, D. A new approach to detecting vegetation and land-use Change using high-resolution lipid biomarker records in stalagmites. *Quat. Res.* **2007**, *68*, 314–324. [[CrossRef](#)]
16. Xing, L.; Zhao, m.; Gao, W.; Wang, F.; Zhang, H.; Li, L.; Liu, J.; Liu, Y. multiple proxy estimates of source and spatial variation in organic matter in surface sediments from the southern Yellow Sea. *Org. Geochem.* **2014**, *76*, 72–81. [[CrossRef](#)]
17. Poerschmann, J.; Koschorreck, m.; Gorecki, T. Organic matter in sediment layers of an acidic mining lake as assessed by lipid analysis. Part II: Neutral lipids. *Sci. Total Environ.* **2016**, *578*, 219–227. [[CrossRef](#)]
18. Guo, W.; Jia, G.; Ye, F.; Xiao, H.; Zhang, Z. Lipid biomarkers in suspended particulate matter and surface sediments in the Pearl River Estuary, a subtropical estuary in southern China. *Sci. Total Environ.* **2019**, *646*, 416–426. [[CrossRef](#)]
19. Zhang, Y.; Su, Y.; Liu, Z.; Sun, K.; Kong, L.; Yu, J.; Jin, m. Sedimentary lipid biomarker record of human-induced environmental change during the past century in Lake Changdang, Lake Taihu basin, Eastern China. *Sci. Total Environ.* **2017**, *613–614*, 907–918. [[CrossRef](#)]
20. Meyers, P.A. Organic geochemical proxies of paleoceanographic, paleolimnologic, and paleoclimatic processes. *Org. Geochem.* **1997**, *27*, 213–250. [[CrossRef](#)]
21. Jiang, Q.; Li, S.; Chen, Z.; Huang, C.; Wu, W.; Wan, H.; Hu, Z.; Han, C.; Zhang, Z.; Yang, H.; et al. Disturbance mechanisms of lacustrine organic carbon burial: Case study of Cuopu Lake, Southwest China. *Sci. Total Environ.* **2020**, *746*, 140615. [[CrossRef](#)] [[PubMed](#)]
22. Huang, S.; Pu, J.; Li, J.; Zhang, T.; Cao, J.; Pan, m. Sources, variations, and flux of settling particulate organic matter in a subtropical karst reservoir in Southwest China. *J. Hydrol.* **2020**, *586*, 124882. [[CrossRef](#)]
23. Pu, J.; Li, J.; Zhang, T.; martin, J.B.; Yuan, D. Varying thermal structure controls the dynamics of CO<sub>2</sub> emissions from a subtropical reservoir, south China. *Water Res.* **2020**, *178*, 115831. [[CrossRef](#)] [[PubMed](#)]
24. Huang, S.; Pu, J.; Cao, J.; Li, J.; Zhang, T.; Jiang, F.; Li, L.; Wu, F.; Pan, m.; Bai, B. Origin and effect factors of sedimentary organic carbon in a karst groundwater-fed reservoir, South China. *Environ. Sci. Pollut. Res. Int.* **2018**, *25*, 8497–8511. [[CrossRef](#)]
25. Li, J.; Pu, J.; Zhang, T.; Huang, S.; Yuan, D. Seasonal variations and intricate diel differences in the physio-chemical parameters and CO<sub>2</sub> emissions from a typical karst groundwater-fed reservoir in southern China. *Environ. Earth Sci.* **2019**, *78*, 484. [[CrossRef](#)]
26. Zhang, T.; Li, J.; Pu, J.; Li, R.; Wu, F.H.; Li, L. Experimental study on the utilization efficiency of Chlorella to Ca<sup>2+</sup> and HCO<sub>3</sub><sup>-</sup> in karst water. *Carsol. Sin.* **2018**, *37*, 81–90.
27. Xin, S.L.; Liang, Y.M.; Peng, W.J.; Song, A.; Jin, Z.J.; Zhu, m.N.; Li, Q. Relationship Between the Bacterial Abundance and Production with Environmental Factors in a Subtropical Karst Reservoir. *Huan Jing Ke Xue* **2018**, *39*, 5647–5656.
28. Elias, V.O.; Cardoso, J.N.; Simoneit, B.R.T. Acyclic Lipids in Amazon Shelf Waters. *Estuar. Coast. Shelf Sci.* **2000**, *50*, 231–243. [[CrossRef](#)]
29. Fang, J.; Wu, F.; Xiong, Y.; Li, F.; Du, X.; An, D.; Wang, L. Source characterization of sedimentary organic matter using molecular and stable carbon isotopic composition of n-alkanes and fatty acids in sediment core from Lake Dianchi, China. *Sci. Total Environ.* **2014**, *473–474*, 410–421. [[CrossRef](#)]
30. Liu, H.; Liu, W. n-alkane distributions and concentrations in algae, submerged plants and terrestrial plants from the Qinghai-Tibetan Plateau. *Org. Geochem.* **2016**, *99*, 10–22. [[CrossRef](#)]
31. Dunstan, G.; Volkman, J.; Barrett, S.; Garland, C. Changes in the lipid composition and maximisation of the polyunsaturated fatty acid content of three microalgae grown in mass culture. *J. Appl. Phycol.* **1993**, *5*, 71–83. [[CrossRef](#)]
32. Ficken, K.J.; Li, B.; Swain, D.L. An n-alkane proxy for the sedimentary input of submerged/floating freshwater aquatic macrophytes. *Org. Geochem.* **2000**, *31*, 745–749. [[CrossRef](#)]

**Disclaimer/Publisher's Note:** The statements, opinions and data contained in all publications are solely those of the individual author(s) and contributor(s) and not of MDPI and/or the editor(s). MDPI and/or the editor(s) disclaim responsibility for any injury to people or property resulting from any ideas, methods, instructions or products referred to in the content.